

1 **Which perceptual categories do observers experience during multistable**
2 **perception?**

3

4

5 Jan Skerswetat * ^{1,2} & Peter J. Bex ²

6

7

8 ¹ Department of Ophthalmology, University of California-Irvine, 850 Health Sciences Road,
9 Irvine, 9269, United States of America

10 ² Department of Psychology, Northeastern University, 360 Huntington Ave, Boston, Massachusetts,
11 02115, United States of America

12

13 Jan Skerswetat: <https://orcid.org/0000-0002-2470-8404>

14

15 Corresponding Author *

16 Email address: jskerswe@hs.uci.edu

17

18

19

20

21

22

23

24

25

26

27

28

29

30

31

32

33

34 **Abstract**

35 Multistable perceptual phenomena provide insights into the mind's dynamic states
36 within a stable external environment and the neural underpinnings of these
37 consciousness changes are often studied with binocular rivalry. Conventional methods
38 to study binocular rivalry suffer from biases and assumptions that limit their ability to
39 describe the continuous nature of this perceptual transitions and to discover what kind
40 of percept was perceived across time. In this study, we propose a novel way to avoid
41 those shortcomings by combining a continuous psychophysical method that estimates
42 introspection during binocular rivalry with machine learning clustering and transition
43 probability analysis. This combination of techniques reveals individual variability and
44 complexity of perceptual experience in 28 normally sighted participants. Also, the
45 analysis of transition probabilities between perceptual categories, i.e., exclusive and
46 different kinds of mixed percepts, suggest that interocular perceptual competition,
47 triggered by low-level stimuli, involves conflict between monocular and binocular
48 neural processing sites rather than mutual inhibition of monocular sites.

49

50 **Keywords**

51 Visual consciousness, perceptual categories, unsupervised machine learning,
52 binocular rivalry, multistable perception

53

54 **Layman abstract**

55 When our brain receives ambiguous information about the world, it changes its
56 interpretation between different alternatives and thereby provides insight into how the
57 mind works. Scientists often use a technique called binocular rivalry, where each eye
58 sees a different image, to provoke an ambiguous visual world that is perceived as
59 ongoing competition among interpretations of the two eyes inputs. Traditional methods
60 for studying binocular rivalry struggle to describe the continuous nature of this
61 fluctuation and to estimate the range of different perceived experiences. We have
62 created a new approach in which participants reproduce their ongoing perceptual
63 experiences combined machine learning analyses of these states. We found that
64 individuals visual experience is more varied and complex than previously thought. Our
65 results suggest that when our eyes see conflicting images, the brain's effort to make
66 sense of what is seen involves syntheses among both monocular and binocular brain
67 areas, not just competition between monocular areas.

68 Introduction

69 The quest to understand consciousness has seen a boom of visual paradigms to
70 investigate the relationship between awareness and neural correlates. Methods that
71 provoke endogenous multistable perceptual competition without exogenous stimulus
72 change have become prominent tools to investigate changes of the contents of visual
73 consciousness over time in the minds of humans (1) and other primates. (2) In one
74 multistability paradigm, when different images are presented to each eye viewers
75 typically experience *binocular rivalry* and perceive transitions among the image
76 presented to the left eye (left exclusivity), the image presented to the right eye (right
77 exclusivity) and mixtures of those images (including superimposition and piecemeal
78 combinations). The measurement of binocular rivalry has the potential to identify
79 clinical biomarkers of neuro-atypicality (3) and personality traits. (4)

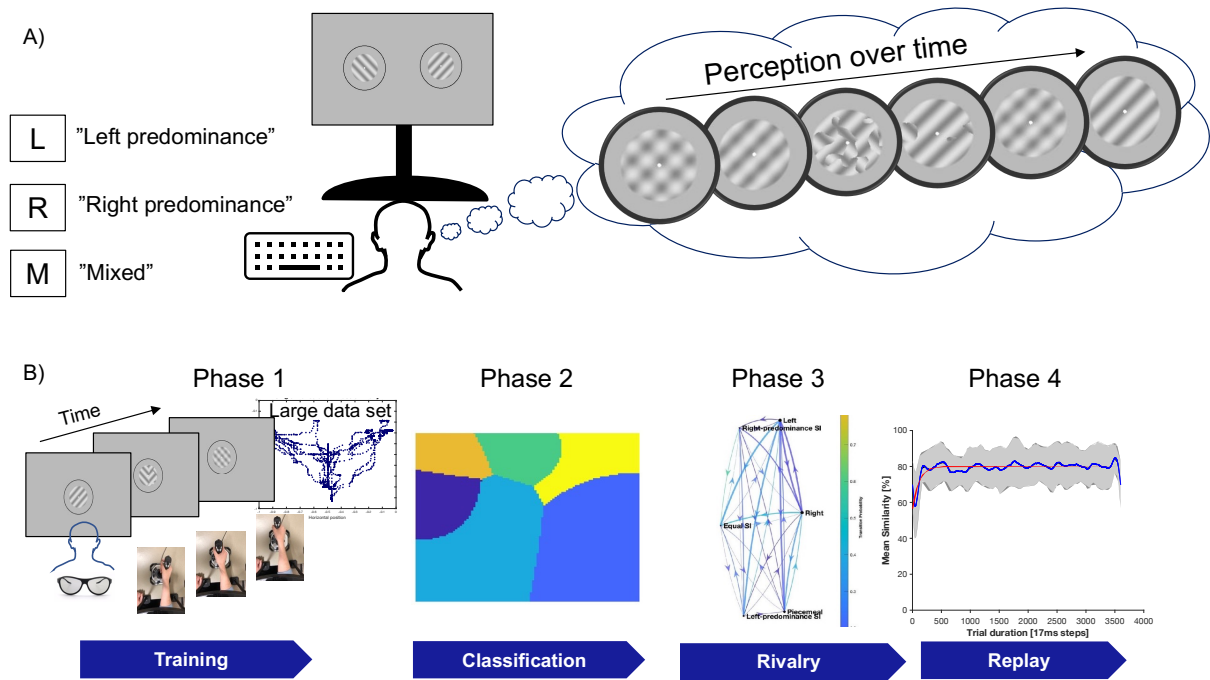
80 A well-known problem with the study of these correlates of conscious experience is
81 that the gradual nature of perceptual changes is not well-captured with standard
82 paradigms that are used to measure multistability. During conventional alternative-
83 forced-choice (AFC) tasks, the observer is instructed to classify moment-to-moment
84 changes in their subjective experiences typically by pressing buttons assigned to
85 different perceptual categories. The available categories are pre-selected by the
86 experimenter, are often only described verbally, and have included two exclusive
87 percepts (2 AFC), (5) two exclusive percepts and all mixed percepts (3 AFC, see
88 Figure 1A), (6) two exclusive and two mixed (piecemeal and superimposed) percepts
89 (4 AFC), (7) two exclusive and three mixed (left-predominant, right-predominant or
90 equal superimposition) percepts (5 AFC). (8) The instructions for the perceptual
91 categorization given by the experimenter may further vary between 'predominance' (9)
92 and 'exclusivity' (10) within each category and even lead to additional judgement
93 criterion of proportions within any moment of viewing (e.g. $\geq 75\%$ predominance (11)).
94 These methods do not provide validated, personalized estimation of perceptual states
95 or their boundaries, make assumption that the experiences described by the
96 experimenter represent the experiences for the participant, do not capture all mixed
97 perceptual experiences reported in the literature, button press methods provide are
98 low in data resolution, nor are they able to track perceptual experiences within mixed
99 categories (piecemeal and superimposition). For further review on rivalry methods
100 please see. (12)

101
102
103
104
105
106
107
108
109
110
111
112
113
114
115
116
117
118
119
120
121
122
123
124
125
126
127
128
129
130

Concerns that the active report requirement of AFC paradigms may unintentionally influence conscious experience have been addressed by no-report paradigms. In these approaches, an observer performs a binocular rivalry task twice: once with and once without an AFC button pressing task while pupil diameter, (13) optokinetic nystagmus, (14) or active gaze changes are simultaneously recorded. (15) The ocular biomarkers are then correlated with the participants' behavioral indications and used to classify experiences with or without active indication of behavior. However as no-report paradigms relied on conventional AFC methods, they too suffer the same limitations and have a number of other confounders e.g., pupil size changes used as no-report biomarker can be affected by different perceptual states regardless of perceptual alternation, or that eye-movements may be triggered due to piecemeal rather than exclusive percepts. (15,16)

Notice that all the above methods rely on two or more pre-defined categories for the participant to report by AFC and are based on the assumption that the categories defined by the experimenter are the same as those experienced by all participants. This assumption may be false, especially for atypical populations. Furthermore, the dynamics of transitions among states cannot be measured sensitively with button responses, which can only indicate abrupt transitions. Furthermore, these methods do not estimate an observer's interpretation of the experimenter's description of categorical boundaries, e.g. "exclusive left-tilt", "piecemeal" etc. (see (17) for review of methods).

To address these shortcomings, we recently developed a continuous method called *Indicate-Follow-Replay Me: Binocular rivalry* (InFoRM: Rivalry) that can generate *a priori* personalized estimates of perceptual introspection and captures the dynamics of perceptual changes. The data can also be re-analyzed between and within perceptual categories that have been used in previous studies. The endogenous changes in perceptual experience reported with InFoRM are validated against exogenous changes via a physical replay of stimuli (Figure 1B). (17)



131

132

133

134

135

136

137

138

139

140

141

142

143

144

145

146

147

148

149

150

151

152

Figure 1: Scheme for different binocular rivalry paradigms. A) Scheme of typical binocular rivalry setting. When an observer views dissimilar stimuli, e.g., achromatic sinusoidal gratings tilted -45° and $+45^\circ$ viewed dichoptically, perceptual competition arises in which experiences gradually change across time, known as binocular rivalry. The traditional task for the observer is then to continuously report what is seen via key presses assigned to categories by an experimenter, here a 3-Alternative-Forced-Choice task. B) Schematic overview of the InFoRM: Rivalry paradigm. During Indicate-Me (Phase 1), participants explore the stimulus-space, moving a joystick to modify binocular-non-rivaling stimuli in real-time that generate corresponding changes of the physical image. The participants were then asked to move the joystick to highlight images that they consider representative of six canonical rivalry states ('exclusive left-tilted', 'exclusive right-tilted', 'piecemeal', 'equal superimposition', 'superimposition with left-tilted predominance', and 'superimposition with right-tilted predominance'), that have been reported in previous rivalry literature. During Follow-Me (Phase 2), participants moved the joystick to match perceptual reports for physically changing binocular-non-rivaling-stimuli to confirm their understanding of the relationship between the joystick position and stimulus appearance. Participants followed four trials that reproduced the rivalry experiences of author JS and four trials that reproduced the six rivalry states the participant had generated themselves during phase 1 - Indicate-Me. This trained participants to track their changing experiences during perceptual rivalry while also capturing the participant's joystick position for each

153 of six canonical perceptual categories. These data used to build estimates of
154 introspection for each category, indicated with different colors in the classification
155 figure. During Rival-Me (Phase 3), participants reported their perception with the same
156 instruction as for Phase 2. The resulting data were then analyzed with various
157 techniques, including the illustrated Hidden Markov Models. During Replay-Me (Phase
158 4), participants' responses during the Phase 3-Rival-Me dichoptic-trials were used to
159 generate physically changing binocular stimuli, that the participant again tracked which
160 validated their individual perceptual-state-space. These data from Phase 3 and Phase
161 4 were then analyzed for similarity illustrated by the plot for one representative
162 participant.

163

164 The InFoRM method allows us to address many questions that cannot be studied with
165 current approaches. For example, rather than assuming each participant experiences
166 2 or more pre-specified categories, we can examine *a priori* how many distinct
167 categories were reported for each participant and experimental condition. In the
168 present study, we investigated three contrast conditions that are known to affect
169 binocular rivalry: bilateral low, bilateral high, and low versus high contrasts, see more
170 details here.⁽¹⁷⁾ To determine the *a priori* categories first, data for each trial,
171 participant, and contrast condition were analyzed using an unsupervised machine
172 learning approach (k-means), and determined the clusters for a range of 1-10, 25, 50,
173 100, 1000 k-means (example Figure 2A). Then, we measured separation of the
174 clusters using Silhouette analysis (Figure 2B). Next, we used a two-parameter fit to
175 estimate the minimal number of clusters necessary to generate well-separated
176 clusters (Figure 2C) and repeated the procedure for all participants and contrast
177 conditions (Table 1). Finally, we repeated the analysis to validate the method against
178 the physical replay data from Phase 4. As shown in Table 1, averaged across trials,
179 participants, and contrast conditions, perceptual rivalry and physical replay generated
180 10 ± 8 and 10 ± 7 optimal clusters, respectively, which are well-separated (silhouette
181 value 0.62 ± 0.06 and 0.62 ± 0.06).

182

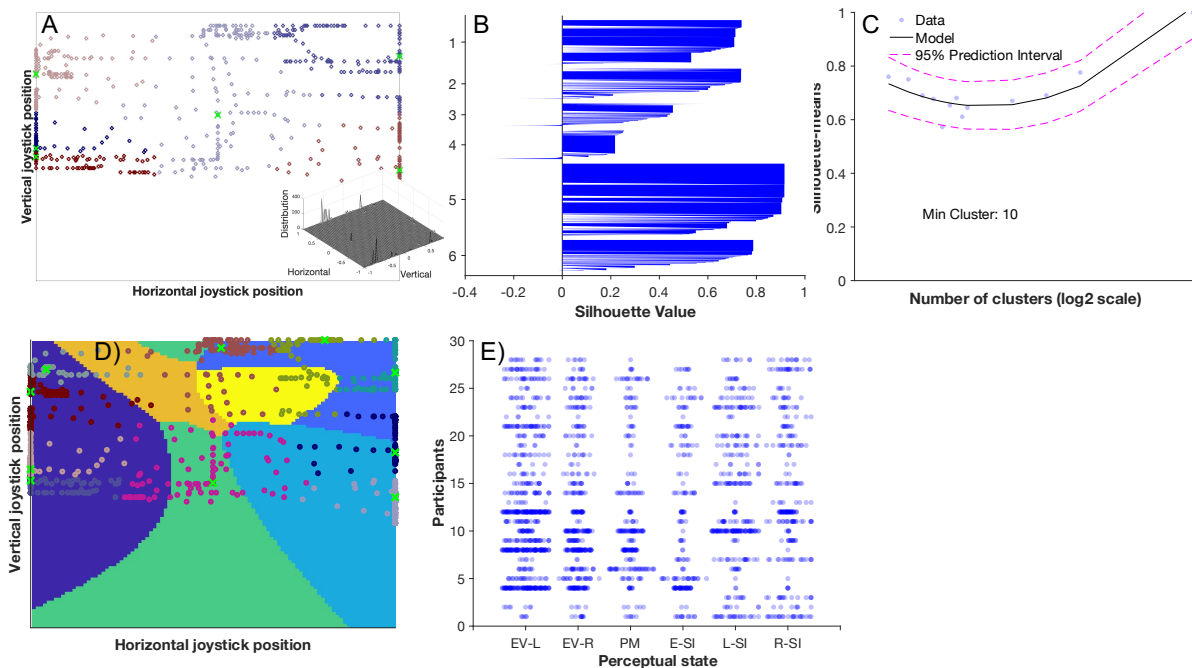
183

184

185 **Table 1: Summary of k-means optimal cluster analysis. Shown are mean and**
 186 **standard deviations across participants outcomes for the minimum silhouette**
 187 **values and their corresponding number of k-mean clusters for joystick report**
 188 **during perceptual and physical stimulus changes.**

Contrast condition	Perceptual Rivalry (Phase 3)		Physical Replay (Phase 4)	
	Min. silhouette value	Min. k value	Min. silhouette value	Min. k value
Low vs. Low	0.64 ±0.055	9 ±7	0.63 ±0.065	10 ±7
High vs. High	0.61 ±0.054	12 ±7	0.61 ±0.059	11 ±8
Low vs. High	0.62 ±0.063	9 ±8	0.64 ±0.075	9 ±7
Mean	0.62 ±0.057	10 ±8	0.62 ±0.060	10 ±7

189



190

191 **Figure 2: Data analysis using unsupervised cluster analysis.** A) Example of
 192 joystick position during a Phase 3 rivalry trial. Depicted are raw data (dots), classified
 193 by k-means clustering illustrated by different colors. The centroid of each cluster is
 194 indicated via green x. B) The same data as in A) plotted with silhouette analysis, the
 195 separation of each data point is expressed with a silhouette value. C) Silhouette values
 196 were calculated for 1-10, 25, 50, 100, 1000 clusters. Then, the mean silhouette was
 197 calculated for each participant and cluster condition (blue dots) and fit with a second
 198 order polynomial (black line, magenta dashed lines show 95% confidence intervals).
 199 The minimum of the function identifies the minimum numbers of clusters, here 10

200 clusters. D) Illustration of raw data from A) with their optimal number of clusters
201 (indicated with different hues) and centroids (green x) superimposed with that
202 individual's perceptual state map generated during phase 2 'Follow me'; (blue-left:
203 exclusive left; green: equal superimposition; beige: superimposition with left-tilted
204 predominance; blue-middle right: piecemeal; blue-upper right: exclusive right; yellow:
205 superimposition with right-tilted predominance). E) Swarm plot of clusters for the low
206 contrast condition for 8 trials for all 28 participants. Individual optimal k-means are
207 superimposed on their perceptual state map, assigning number of k-means centroids
208 for each of six perceptual states (x axis) for each individual (y axis).

209

210 Although individuals were trained on 6 categorical states (based on a review of
211 previous studies), the results show that on average more distinct clusters experiences
212 were perceived during rivalry. Our data allow us to examine the agreement between
213 the six canonical states that are commonly assigned and the 9 or 10 clusters that
214 participants spontaneously report. To answer this question, we return to the
215 introspection maps that were created during InFoRM's Phase 2 and superimposed
216 these with the optimal k-means from Experiment 1 for each participant and condition.
217 These maps were created based on each participant's estimate of each of the six
218 canonical categories previously described in the literature.⁽¹⁷⁾ We assigned each k-
219 means centroid from each trial to the closest of the six canonical categories and
220 repeated this for each contrast condition (see example in Figure 2 D). As show in
221 Figure 2E for the low contrast condition, the number of centroids in each perceptual
222 state region varied between participants and occurred primarily in the *exclusive*
223 portions of the joystick space as well as in the *superimposed* states with predominance
224 of either left or right with fewer reports around *equal superimposition* or *piecemeal*
225 observations during rivalry. These results suggest that *piecemeal* percepts can be
226 thought of as an intermediate phase between both exclusive states (i.e. monocular
227 sites) and superimposed states (binocular site).

228

229 Averaged across trials and participants, 13 ± 9 , 15 ± 10 , 12 ± 11 centroids emerged for
230 the low, high, and low vs. high contrast conditions, respectively, and were not
231 significantly different from each other [repeated measure ANOVA, Greenhouse-
232 Geisser $F(2.0, 53.1) = 1.7$, $p > 0.05$, $\eta_p^2 = 0.06$]. However, as can be seen exemplarily in

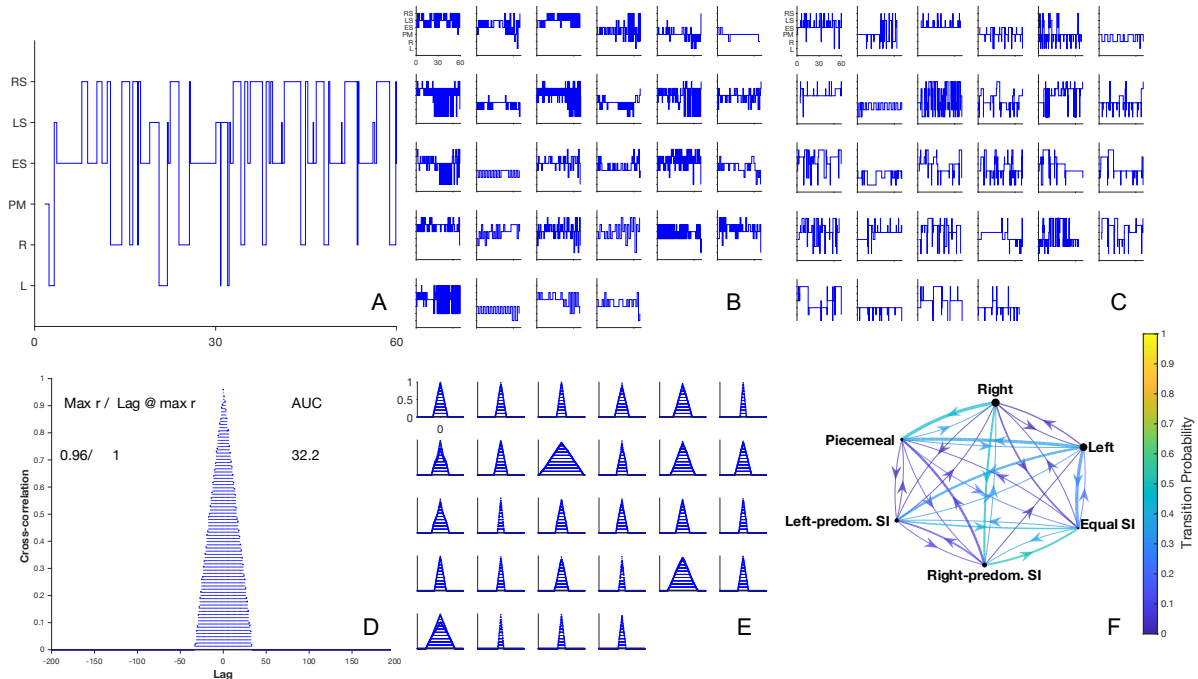
233 Figure 2E for the low contrast condition, the number of centroids across states varied
234 significantly (two-way ANOVA, $[F(3.0,80.0)=14.5, p<0.001, \eta_p^2= 0.35]$) but not was not
235 affected by the contrast condition $[F(2.0,53.1)=1.7, p>0.05, \eta_p^2= 0.06]$.

236 We calculated the size of each classified area, as shown in Figure 2E, to investigate
237 the relative sizes of different perceptual states. Averaged across trials, participants
238 and contrast, the six states occupied $23\% \pm 4$, $16\% \pm 5$, $25\% \pm 7$, $9\% \pm 7$, $12\% \pm 3$, 15%
239 ± 3 and showed a significant difference. (17) The number of cluster centroids falling
240 within the 6 classic categories, averaged across all levels, was 22 (exclusive left 27%
241 of all clusters) ± 25 , 14 (exclusive right, 17%) ± 15 , 9 (piecemeal, 11%) ± 13 , 6 (equal,
242 7%) ± 8 , 19 (left-predominant superimposition, 24%) ± 23 , 10 (right-predominant
243 superimposition, 14%) ± 13 . Interestingly, these results show that area and number of
244 clusters mismatch for piecemeal and predominant left superimposed areas. In fact,
245 although the piecemeal area of the introspection maps was the largest classification
246 area overall, it housed only a small proportion of clusters. Taken together, a
247 considerable number of clusters are generated in superimposed mixed states that
248 resulted in 35% of all superimposed experiences and 12% piecemeal perception as
249 reported previously. (17) These results suggest that current standard 2-3AFC methods
250 have neglected these superimposed categories and thus may not accurately represent
251 the experiences or their underlying neural site(s). Some studies have reported
252 superimposition as a perceptual category during binocular rivalry, (18,19) but only a
253 few used 4-5AFC methods to investigate the perceptual dynamics during binocular
254 rivalry. (7,8) Only two studies have reported explicit experiences of superimposition
255 with a predominance one eye's stimuli. In one case it was invoked due to difference
256 in spatial frequency (20) in the other it was invoked using the same spatial frequency
257 but varying unilateral and bilateral stimulus contrasts. (17) Our results show that, even
258 with bilateral equal stimuli, these experiences can emerge. It may be possible that
259 studies that used ambiguous instructions such as 'predominance' may have captured
260 instances of these experiences as well. (21,22) Importantly, while exclusive perception
261 (global) and piecemeal (local) are thought to be a result of mutual inhibition of
262 monocular sites, (23) superimposed percepts may activate distinct neural correlates
263 (24) that might include binocular cells as suggested by different psychophysical
264 investigations. (7,8,18)

265

266 In addition to investigating the categorical experiences during binocular rivalry, we
267 next interrogate the transitory dynamics among these experiences during binocular
268 rivalry.

269



270

271 **Figure 3: Analysis of binocular rivalry dynamics.** A) A typical transition path of a
272 single trial for one participant classified into 6 classic perceptual states ('L' left-tilted
273 exclusive, 'R' right-tilted exclusive, 'PM' piecemeal, 'ES' equal superimposition, 'LS'
274 left-tilted predominant superimposition, 'RS' left-tilted predominant superimposition)
275 changes across time. B) Mean transition path for each participant during the low
276 contrast conditions were then used to estimate the most likely transition path (C)
277 calculated by a hidden Markov model. D) Cross-correlation for one participant as a
278 function of lag between actual and model data. Maximum correlation coefficient, r , and
279 its lag location relative to the optimum 0 lag as well as the estimated area under the
280 curve (AUC) are included. E) Cross-correlations for each individual during the low
281 contrast condition. F) Transition probability chain plot averaged across trials and
282 participants for the low contrast condition.

283

284 First, the actual transition path for each trial (example in Figure 3A) was used to
285 calculate the mean transition pathway (Figure 3B) for each participant and condition.
286 Then, the most likely transition pathway for each participant and condition was
287 estimated using a Hidden Markov Model (Figure 3C). Next, the similarity of the model

288 with the actual data was estimated by using cross-correlation to determine the
289 agreement between the model and data (Figure 3D). The resulting similarity measures
290 (maximum correlation coefficient, lag at maximum correlation, and area under the
291 curve) were further analyzed. Separate repeated measure ANOVAs were performed
292 to test for an effect of contrast condition. An effect for area under the curve
293 [$F(1.8,48.0)=2.8$, $p<0.01$, $\eta_p^2=0.21$] was found due to less AUC for the high vs low
294 contrast condition. Maximum correlation coefficient [$F(1.7,46.3)=1.4$, $p>0.05$, $\eta_p^2=$
295 0.05], nor for lag at maximum correlation (bias) [$F(1.0,27.0)=1.0$, $p>0.05$, $\eta_p^2=0.04$]
296 was found. The lag at maximum correlation was close to zero (1 ± 0.11).

297

298 Previously, we introduced a new way to analyze multistability data, which combines
299 Markov chains and their ability to depict states, their connections, and the likelihood
300 of each connection with the temporal priors, i.e., the mean duration of a percept before
301 it transitioned to another state (indicated via arrow thickness, where arrow thickness
302 increases with percept duration) and the mean duration of each principal state (nodes,
303 where diameter increases with mean duration (3)). This method therefore makes
304 predictions of state connections and their likelihoods and also incorporates temporal
305 legacy of each of these transitions. The node diameters (Figure 3F) symbolize each
306 state's mean duration, each arrow thickness (weights) indicates the mean duration of
307 a given perceptual state prior to transition to another state. We correlated the weights
308 with the transition probability values for each contrast condition and found no
309 correlation for the low ($R: 0.01$; $p>0.05$) or high contrast conditions ($R: 0.13$; $p>0.05$),
310 but a positive correlation when using different dichoptic contrasts i.e., the longer the
311 prior duration of percepts the greater the transition likelihood between these two
312 perceptual categories ($R: 0.39$; $p<0.05$). On one hand, these results imply that when
313 using equal bilateral contrasts, rivalry transition dynamics are not dependent upon
314 prior accumulative experiences (weights), suggesting a primary role of intrinsic noise
315 as driver for transition. (25) On the other hand, the positive correlation between
316 weights and transition probabilities when using unequal bilateral contrasts suggest a
317 role of prior experience, supporting the hypothesis that this type of multistable vision
318 is explained by self-adaptation models. (26)

319 We compared probability distributions between contrast conditions using a Kullback
320 Leibler divergence. As expected, when comparing the dissimilarity of transition

321 probabilities for the equal bilateral contrast conditions (low/low vs. high/high),
322 dissimilarity was the lowest (range: 0.05-0.29), whereas dissimilarity was higher for
323 unequal bilateral contrast conditions (low vs. low/high conditions [0.11-0.50]; and high
324 vs. low/high conditions [0.14-0.57]). As illustrated for the bilateral low contrast
325 condition in Figure 3F, changes away from exclusive states to predominant-
326 superimposed states are more likely and with longer mean durations (thicker arrows)
327 compared to other changes. One hypothetical reason for this result could be the
328 joystick arrangement i.e., left tilt for left exclusive and right tilt for right-exclusive
329 percepts, however, as shown in Figure 3B and 3C, mixed states were not mere transit-
330 states between two exclusive percepts for the majority of participants. As for data
331 clustering, we show considerable individual differences in transition dynamics
332 between perceptual states. Furthermore, the analysis reveals a higher transition
333 probability between exclusive and left and right-predominance superimposed states.
334 Specifically, for the low contrast condition the minimum transition probability 0 (no
335 transition from left exclusive to right predominant superimposition, SI); maximum 0.50
336 (right predominant SI to equal SI), and a mean of 0.19. The results for high contrast
337 [*min*: 0.007;(exclusive right to equal SI); *max*:0.50 (right-tilted SI to equal SI), *mean*:
338 0.18] and for the low versus high contrast conditions [*min*: 0.01(low contrast to high-
339 contrast predominant SI); *max*: 0.50 (low contrast to low contrast predominant SI);
340 *mean*: 0.19] indicate that transitions were more likely to occur between exclusive
341 monocular and fused binocular percepts.

342

343 In conclusion, the combination of a continuous psychophysical approach,
344 introspection estimates, and unsupervised cluster analysis revealed that on average
345 more perceptual categories arise during binocular rivalry than previously thought.
346 Moreover, binocular rivalry transitions are more likely to occur between exclusive and
347 superimposed perceptual states than other state changes and are affected by prior
348 experiences only when the interocular inputs are different. Together, these results
349 suggest that conventional binocular rivalry paradigms do not capture the full range of
350 experiences during binocular rivalry or their dynamics. Furthermore, transitions among
351 states show greater variability than previously thought, in particular within
352 superimposed perceptual categories. The results of the transition probability analysis
353 imply that perceptual competition during binocular rivalry that is evoked by low-level

354 stimuli arises as a conflict between monocular and binocular neural sites rather than
355 mutually inhibiting monocular sites.

356

357 **Methods**

358

359 The experiments were carried out in the facilities of Northeastern University, Boston.
360 Written and verbal information about the project were provided in advance to the
361 participants and they gave written informed consent before taking part. Ethics approval
362 to conduct the experiments on human participants was in line with the ethical principles
363 of the Helsinki declaration of 1975 and ethics board of the Northeastern University.
364 The methods regarding the InFoRM Rivalry method have been reported elsewhere in
365 detail. (17) Here we report methods and materials specific to the data analysis. Matlab
366 (Mathworks, version 2023b) was used for data collection, analysis, and visualization
367 of the results in the current study. Stimuli were presented on a LG 3D polarized
368 monitor with a spatial resolution of 1920*1080 pixels in combination with radially-
369 polarized LG cinema 3D glasses (AG-F310), 60Hz refresh rate and mean luminance
370 of 61.9 cd/m², and a Dell computer (Optiplex 7060). The viewing distance was 150cm.
371 The participants wore radially-polarized LG cinema 3D glasses (AG-F310) and
372 provided responses with a Logitech Extreme™ 3D pro (Logitech Europe S.A.)
373 joystick.

374

375 Binocular rivalry was induced in 28 normally-sighted participants using orthogonally
376 oriented ($\pm 45^\circ$) sinusoidal gratings ($2^\circ \varnothing$, $2c/^\circ$). Three contrast conditions (low versus
377 low; high versus high, and high versus low) were tested in counterbalanced order.
378 Raw data consisted of 3600 data points (60Hz joystick data sampling * 60seconds
379 testing; 16.7ms temporal resolution) per trial (8 per contrast condition) that consisted
380 of 2D joystick position estimates for each Phase 3 (rivalry) and Phase 4 (replay) and
381 were stored in .mat files. Perceptual introspection maps and state assignment during
382 Phase 3 (rivalry) and Phase 4 (replay) were described elsewhere. (17)

383

384 **Cluster Analysis**

385

386 Horizontal and vertical joystick vectors were converted into Euclidean space for the
387 Phase 3 (rivalry) data for each trial. Second, unsupervised clustering was performed
388 for a range of clusters (1-10, 25, 50, 100, 1000) using the *kmeans* function applying
389 the ‘cityblock’ method for each trial and averaging the results across trials for each
390 condition. Third, we evaluated the separation among clusters using the *silhouette*
391 function and applied again the ‘cityblock’ method. We found that the overall silhouette
392 values were all positive, i.e. well-separated. As the choice of k-means is arbitrary, we
393 decided to find the minimum separation value required, which represents the optimal
394 clustering value. Hence, for the fourth step, we plotted the resulting silhouette values
395 against k-means for each participant and for each condition, fit a quadratic function
396 using *polyfit* and *polyval* functions to the data to estimate the minima of the fit, and
397 extracted the corresponding optimal silhouette value and optimal number of k-means
398 clusters. We repeated the above-described analysis for Phase 4 (replay).
399 Each participant's optimal k-means value was used for the assignment to their
400 respective introspection maps to find out where within the classification space the
401 centroids would cluster. Then, we assigned each centroid for each trial with one of the
402 six introspection classifications derived from previous binocular rivalry studies. For
403 example, if a centroid arose in the introspection map area of ‘left exclusive”, that
404 centroid was counted for left exclusive. This was repeated for each trial, participant,
405 and contrast condition. SPSS software (IBM, version 28.0.0.0.(190)) was used to
406 perform repeated measure ANOVAs.

407

408 **Transition Probability Analysis**

409

410 *Actual and HMM most likely transition path*

411 Each trial's perceptual state vector (3600 data) consisted of up to six distinct states
412 and was averaged across trials for each participant to generate the average transition
413 path. The *hmmestimate* function was used to calculate the mean transition probability
414 for that trial. The *hmmestimate* function was repeated with the ‘pseudotransition’
415 setting using the mean transition value as some transition probabilities were very low.
416 Next, the HMM most probable transition path for each trial was estimated using the
417 *hmmviterbi* function. Single transition paths were visualized using the *stairs* function.

418 *Cross correlation of Actual and HMM transition path*

419 The *xcorr* function ('normalized' mode, maximum lag of ± 200 time points = ± 3.3
420 seconds) was used for the cross correlation of the actual mean paths and means of
421 the most likely paths HMM paths for each participant, and contrast condition. The peak
422 of the resulting cross correlation function, lag, and area under the curve (estimated
423 using the *trapz* function) were taken.

424 *Markov chains*

425 The *hmmestimate* function was used to estimate the transition likelihoods between
426 states for each trial, participant, and contrast condition. We used the *dtmc* function to
427 estimate Markov chains that were then plotted using the *graphplot* function for each
428 contrast condition.

429 As previously described, (3) we also included temporal legacy in the chain plot,
430 indicated by increasing node diameter for mean durations and thicker arrows (weights)
431 for longer prior mean durations before a transition occurred. Each weight was
432 measured for each trial as a mean duration of how long either of the six canonical
433 perceptual states lasted. The results were then averaged across trials and participants
434 for each contrast condition. The *corrplot* function using Pearson's method was applied
435 for linear correlations between weights and transition probabilities, testing for R and
436 for statistical significance test p. Kullback-Leibler similarity analysis was performed to
437 compare the transition probabilities between contrast conditions applying the *KLDiv*
438 function.

439

440

441 **Acknowledgment**

442

443 Supported by NIH grants R01 EY029713 and R01 EY032162 .

444 **Authors contributions**

445 JS and PB developed the principal concept of the study and invented the InFoRM
446 method. Both authors developed and refined the code of the four phases. Both authors
447 contributed to the experimental design of the study. JS and a research assistant
448 carried out the optometric screening and collected data. JS wrote the analysis code

449 and the first draft of the manuscript. Both authors critically revised both code and the
450 manuscript before submission.

451

452 **Competing interests**

453 InFoRM was invented by PJB and JS and is disclosed as patent (pending) held by
454 Northeastern University, Boston USA.

455

456 **Financial interests**

457 Both authors are founders and shareholders of the company PerZeption Inc. (USA)
458 which has licensed the patent for InFoRM.

459

460 **Data availability**

461 Data generated for this study and code can be found here:
462 **10.5281/zenodo.13831435.**

463

464 **References**

465

- 466 1. Blake R, Logothetis NK. Visual competition. *Nat Rev Neurosci*. 2002
467 Jan;3(1):13–21.
- 468 2. Logothetis NK. Single units and conscious vision. *Philos Trans R Soc Lond B*
469 *Biol Sci*. 1998 Nov 29;353(1377):1801–18.
- 470 3. Skerswetat J, Bex, Peter J, Baron-Cohen S. Visual consciousness dynamics in
471 adults with and without autism. *Sci Rep*. 2022;1–27.
- 472 4. Spiegel A, Mentch J, Haskins AJ, Robertson CE. Slower Binocular Rivalry in
473 the Autistic Brain. *Current Biology*. 2019;29(17):2948-2953.e3.
- 474 5. Kang M. Size matters: A study of binocular rivalry dynamics. *J Vis*. 2009;9:1–
475 11.
- 476 6. Yu K, Blake R. Do recognizable figures enjoy an advantage in binocular
477 rivalry? *J Exp Psychol Hum Percept Perform*. 1992 Nov;18(4):1158–73.
- 478 7. Skerswetat J, Formankiewicz MA, Waugh SJ. More superimposition for
479 contrast-modulated than luminance-modulated stimuli during binocular rivalry.
480 *Vision Res*. 2018;142:40–51.
- 481 8. Sheynin Y, Proulx S, Hess RF. Temporary monocular occlusion facilitates
482 binocular fusion during rivalry. *J Vis*. 2019;19(5):23.

- 483 9. Alais D, Blake R. Grouping visual features during binocular rivalry. *Vision Res.* 1999 Oct;39(26):4341–53.
484
- 485 10. Dieter KC, Sy JL, Blake R. Individual differences in sensory eye dominance
486 reflected in the dynamics of binocular rivalry. *Vision Res.* 2017;141:40–50.
- 487 11. Hudak M, Gervan P, Friedrich B, Pastukhov A, Braun J, Kovacs I. Increased
488 readiness for adaptation and faster alternation rates under binocular rivalry in
489 children. *Front Hum Neurosci.* 2011 Jan;5(November):128.
- 490 12. Skerswetat J, Bex PJ. InFoRM (Indicate-Follow-Replay-Me): A novel method
491 to measure perceptual multistability dynamics using continuous data tracking
492 and validated estimates of visual introspection. *Conscious Cogn [Internet].*
493 2023;107(April 2022):103437. Available from:
494 <https://doi.org/10.1016/j.concog.2022.103437>
- 495 13. Schütz I, Busch JE, Gorka L, Einhäuser W. Visual awareness in binocular
496 rivalry modulates induced pupil fluctuations. *J Cogn.* 2018;1(1):1–10.
- 497 14. Naber M, Frässler S, Einhäuser W. Perceptual Rivalry : Reflexes Reveal the
498 Gradual Nature of Visual Awareness. *PLoS One.* 2011;6(6):1–12.
- 499 15. Hesse JK, Tsao DY. A new no-report paradigm reveals that face cells encode
500 both consciously perceived and suppressed stimuli. *Elife.* 2020;9:1–20.
- 501 16. Overgaard M, Fazekas P. Can No-Report Paradigms Extract True Correlates
502 of Consciousness? *Trends Cogn Sci.* 2016;20(4):241–2.
- 503 17. Skerswetat J, Bex PJ. InFoRM (Indicate-Follow-Replay-Me): A novel method
504 to measure perceptual multistability dynamics using continuous data tracking
505 and validated estimates of visual introspection. *Conscious Cogn.*
506 2023;107(103437).
- 507 18. Liu L, Tyler CW, Schor CM. Failure of Rivalry at low contrast: evidence of a
508 suprathreshold binocular rumination process. *Vision Res.* 1992;32(8):1471–9.
- 509 19. Klink PC, Brascamp JW, Blake R, van Wezel RJA. Experience-driven plasticity
510 in binocular vision. *Current Biology.* 2010 Aug 24;20(16):1464–9.
- 511 20. Yang Y, Rose D, Blake R. On the variety of percepts associated with dichoptic
512 viewing of monocular stimuli. *Perception.* 1992;21:47–62.
- 513 21. Sobel K V, Blake R. How context influences predominance during binocular
514 rivalry. *Perception.* 2012;31(7):813–24.
- 515 22. Polonsky A, Blake R, Braun J, Heeger DJ. Neuronal activity in human primary
516 visual cortex correlates with perception during binocular rivalry. Vol. 3, *Nature*
517 *Neuroscience.* 2000. p. 1153–9.
- 518 23. Blake R, O’Shea RP, Mueller TJ. Spatial zones of binocular rivalry in central
519 and peripheral vision. *Vis Neurosci.* 1992 May;8(5):469–78.
- 520 24. Polonsky A, Blake R, Braun J, Heeger DJ. Neuronal activity in human primary
521 visual cortex correlates with perception during binocular rivalry. *Nat Neurosci.*
522 2000 Nov;3(11):1153–9.
- 523 25. Moreno-Bote R, Rinzel J, Rubin N. Noise-induced alternations in an attractor
524 network model of perceptual bistability. *J Neurophysiol.* 2007 Sep;98(3):1125–
525 39.
- 526 26. Wilson HR. Computational evidence for a rivalry hierarchy in vision. *Proc Natl*
527 *Acad Sci U S A.* 2003 Nov 25;100(24):14499–503.
528